Nanotubes and Nanoribbons in displays, NEMS, and chemical sensors: recent results from First-Principles Quantum Mechanics simulations

A. Maiti*

*Accelrys Inc., 9685 Scranton Road, San Diego, CA 92121

ABSTRACT

Of the myriad of potential application areas commonly associated with Nanotechnology, sensors and displays are two of the closest ones to commercial reality. The two materials systems that have given rise to high hopes in these applications are carbon nanotubes (CNT) and metal-oxide nanoribbons. We have used Accelrys' Density Functional Theory (DFT) code DMol^3 [1] to investigate important properties in both systems.

For CNT-based field-emission displays, we have investigated the effect of adsorbates at the nanotube tip on the emission current. For CNT-based nano-electro-mechanical sensors (NEMS), we have computed the electrical response of CNT under pushing with an AFM tip. For SnO_2 nanoribbons we have investigated binding energies and electron transfer for three types of adsorbates: NO_2, O_2 and CO, and explored implications on sensing characteristics.

Keywords: Nanotubes, Nanoribbons, Displays, NEMS, Chemical Sensors.

1 INTRODUCTION

Realistic application potentials and a steady growth of knowledge following the insightful work of a number of researchers have powered carbon nanotubes [2] into a field of intense activity. A handful of commercial applications appear feasible in the not-too-distant future [3], including: Field Emission-based Flat Panel displays, novel semiconducting devices in microelectronics, hydrogen storage devices, structural reinforcement agents, chemical sensors, and ultra-sensitive electromechanical sensors. At the same time, the simple atomic structure of carbon nanotubes and the high degree of structural purity are allowing accurate computer modeling using a variety of theoretical techniques. We have used Accelrys DFT code DMol^3 [1] to investigate: (1) the effect of adsorbed molecules on the field emission from a metallic nanotube tip, and (2) the effect of mechanical deformation on the electrical conductance of nanotubes.

A major bottleneck to the successful commercialization of nanotube-based technology is the difficulty in controlled synthesis of nanotubes of desired diameter and chirality, and the associated high cost of production. An alternative for many applications is the metal-oxide (ZnO, SnO_2) nanoribbons, which can be produced much more easily than carbon nanotubes. The first major application of nanoribbons is expected to be in the area of chemical sensors for different gas species. Recent experiments with SnO_2 nanoribbons have demonstrated marked changes in the electrical conductance upon adsorption of NO_2, O_2 and CO. We have carried out DMol^3 calculations in order to investigate: (1) the binding configurations and energetics of various adsorbates; and (2) the amount and sign of charge transfer upon chemisorption.

2 EFFECT OF ADSORBATES ON FIELD-EMISSION FROM CNTS

Synthesis of CNTs with length-to-width ratio as large as 10^5 and invention of advanced fabrication methods for generating self-aligned or patterned nanotube films on glass or silicon substrate have pushed CNT-based displays on the verge of commercial reality [4]. Prototype displays have already been demonstrated by several companies and academic research groups. One of the main concerns of a field-emission-based flat-panel display device is to reduce the operating voltage. One way to achieve this is to introduce adsorbates that might effectively lower the ionization potential (IP) and facilitate the extraction of electrons. An important experimental work in this regard was done at Motorola [5], which studied changes in field emission behavior in the presence of various gases, i.e., O_2, H_2 and water vapor. While O_2 and H_2 did not affect the field emission behavior appreciably, adsorbed water was found to significantly enhance the emission current. The effect of water on field emission current was more pronounced at low emission, and there was evidence of stability of water molecules on the nanotube tip at temperatures as high as 900 K. In addition, the enhancement in field emission current was found to be more pronounced with an increase in the amount of water vapor.

In order to understand the difference between H_2 and water on the field-emission properties of carbon nanotubes, we carried out first-principles electronic structure calculations using DMol^3. The nanotube tip was represented by a C_{60} half capping a three-layer stem of a (5, 5) armchair tube, known to be metallic from simple electronic structure arguments. The dangling bonds at the stem end were not saturated with H because the difference in electronegativity between H and C introduces an artificial dipole moment in the nanotube. A uniform external field E_{FE}, directed toward the tube from above, was

chosen to represent the electric field close to the tube tip under field emission conditions. For all calculations a magnitude of E_{FE} = *1 eV/Å* was used as a ballpark figure around which field emission is known to occur for these systems. In order to be consistent with the uniform field representation, the length of the nanotube tip was constrained to be of the order of the tube diameter. The C-atoms at the stem end were frozen during all simulations in order to mimic the presence of a long stem in actual experiments.

There are two stable structures for the H_2 molecule, H_2 (flat) and H_2 (upright), in which the H_2 axis is respectively perpendicular and parallel to the tube axis. The stable structure of water (especially under emission conditions) has its dipole moment parallel to the tube axis, pointing down toward the tube from above. In order to simulate the effect of a higher concentration of water on the tube tip, we have also considered the ground-state geometry of five water molecules, which has a well-defined H-bonded geometry with five-fold symmetry about the tube-axis, as shown in Fig. 1 below.

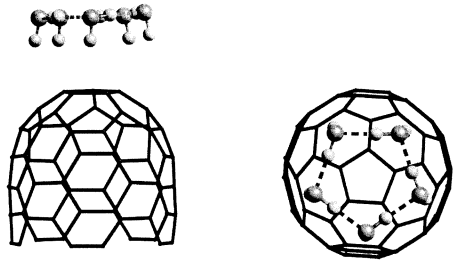

Fig.1. Five-water cluster on nanotube tip (side & top views)

Table 1 (below) lists the binding energies of the various adsorbates, with the binding energy at E = 0 being defined as:

$$E_{binding}[E=0] = E_{CNT}[E=0] + E_{adsorbate}[E=0] - E_{CNT\ +\ adsorbate}[E=0] \quad (1)$$

Therefore, positive binding denotes an exothermic process. It is clear that binding for both H_2 and water is small at E=0, and that no adsorbate would be stable at the tube tip even at room temperature.

However, the above picture of weak interaction in zero fields drastically changes under field emission conditions when large electric fields E_{FE} are present at the tube tip [6]. Since such a field is strongly focussed very close to the tube tip, a sensible definition of binding energy at E_{FE} is as follows:

$$E_{binding}[E=E_{FE}] = E_{CNT}[E=E_{FE}] + E_{adsorbate}[E=0] - E_{CNT\ +\ adsorbate}[E=E_{FE}] \quad (2)$$

$E_{binding}$ in equation (2) can be interpreted as the energy required to detach the adsorbate from the tube tip. This places the adsorbate away from the tip, where the field is negligible compared to E_{FE}. According to the above definition, the binding of the water molecule with the nanotube becomes more than 20 kcal/mol (at E_{FE} = *1 eV/Å*), nearly the strength of a chemical bond. For the 5-water-complex the binding energy is much higher, indicating higher stability on the tip. In contrast, the H_2 molecule has a much weaker binding, more so in the flat configuration, and would not be stable on the tube tip even at room temperatures. This explains why they do not affect the field emission behavior from the tube tip.

Table 1. Binding energies of optimized adsorbate structures on nanotube tip. $E_{binding}$ at E=0 and E=E_{FE} are computed according to Equations (1) and (2) of text.

Adsorbate	$E_{binding}$ (kcal/mol)	
	E = 0	E= E_{FE}
H_2 (flat)	0.0	1.1
H_2 (upright)	0.1	3.5
1 Water	0.7	20.3
5 Water	---	65.0*, 101.4**

* *w.r.t* a relaxed five-water complex at E = 0
** *w.r.t* five isolated water molecules at E = 0

Structural changes and charge transfer are rather small even under large electrostatic forces at E = E_{FE}. The most significant effect of the electric field is to polarize the metallic nanotube, thereby inducing a large dipole moment. This induced dipole moment interacts strongly with the intrinsic dipole moment of polar adsorbates like water, and result in a large binding energy [7].

In order to explain why water adsorption enhances field emission, we have computed the ionization potential for three systems at E_{FE} = *1eV/Å*, i.e., nanotube, (nanotube + 1 adsorbed water), and (nanotube + 5 adsorbed water). The Ionization Potential is defined as the energy difference between a system with a +1 charge (i.e. one less electron) and the original system with zero charge. The lower the IP, easier it is to extract an electron, and higher the expected Field emission current at a given operating voltage. In metallic nanotubes, the "hole" left by an emitted electron recombines almost instantaneously with an incoming electron from the stem side. Therefore, the structure with a +1 charge was frozen at the relaxed geometry for the neutrally charged system. Our results indicate that the presence of a single water molecule lowers the IP by 0.1 eV and the presence of five water molecules lowers the IP by 0.6 eV, as compared with the isolated nanotube. In addition, we find that the position of the HOMO becomes unstable by 0.1 eV and 0.6 eV respectively in the presence of one water and the five-water cluster on the nanotube tip (at *E* =

E_{FE}). This correlates perfectly with the corresponding lowering of the ionization potential. Thus, it appears that a polar adsorbate like water exerts an electrostatic field, which makes the HOMO unstable, thereby making it easier to extract electrons out of nanotube tips and enhancing the field-emission current [7]. In all cases, the HOMO appears to be localized to within the nanotube, thereby indicating that field emission of electrons occur from the nanotubes themselves and not from the adsorbates.

The above results have recently been confirmed in another computational work, which have extended the analysis to a few additional polar adsorbates [8].

3 CNT-BASED NEMS

Interest in the application of carbon nanotubes as electromechanical sensors got a significant boost from the pioneering experiment of Tombler *et al.* [9], in which the middle part of the segment of a metallic nanotube, suspended over a trench, was pushed with an AFM tip. Beyond a deformation angle of ~ 10° the electrical conductance of the tube dropped by more than two orders of magnitude. The effect was found to be completely reversible, i.e., through repeated cycles of AFM-deformation and tip removal, the electrical conductance displayed a cyclical variation with constant amplitude.

O(N) tight-binding calculations [10] show that beyond a critical deformation several C-atoms close to the AFM tip become sp^3-coordinated. The sp^3 coordination ties up delocalized π-electrons into localized σ-states. This would naturally explain the large drop in electrical conductivity, as verified by explicit transport calculations.

To carry out simulations of AFM-deformation, one needs to consider rather long nanotubes consisting of several thousand atoms. Therefore, in this work, we carried out a combination of first-principles DFT ($DMol^3$) and molecular mechanics using the Universal Forcefield (UFF) [11]. Chemical bond reconstruction, if any, is likely to occur only in the highly deformed, non-straight part of the tube in the middle. This prompted us to use a DFT-based quantum mechanical description of the middle part of the tube (~ 100-150 atoms), while the long and essentially straight part away from the middle was described accurately using the Universal Forcefield.

Because of known difference in electronic response of zigzag and armchair tubes to mechanical deformation, we studied a (12, 0) zigzag and a (6, 6) armchair tube, each consisting of 2400 atoms. The AFM tip was modeled by a 6-layer deep 15-atom Li-needle normal to the (100) direction, terminating in an atomically sharp tip. To simulate AFM-tip-deformation, the Li-needle was initially aimed at the center of a hexagon on the bottom-side of the middle part of tube. The Li-needle tip was then displaced by an amount δ toward the tube along the needle-axis, resulting in a deformation angle $\theta = tan^{-1}(2\delta/L)$, L being the unstretched length of the tube. The whole tube was then relaxed by UFF keeping the needle atoms and the end contact regions of the tube fixed [12]. The contact region atoms were fixed in order to simulate an ideal undeformed semi-infinite carbon nanotube lead, and to ensure that all possible contact modes are coupled to the deformed part of the tube. Following the UFF relaxation, a cluster of 132 C-atoms for the (6, 6) and a cluster of 144 C-atoms for the (12, 0) were cut out from the middle of the tubes. These clusters, referred to below as the *QM clusters* (plus the 15 Li-tip atoms of the AFM tip) were further relaxed with $DMol^3$ with the end atoms of the cluster plus the Li-tip atoms fixed at their respective classical positions. In order to cut down on CPU requirements, the DFT calculations were performed using the Harris functional [13].

Once the relaxed structures were obtained using the combined DFT/UFF approach described in the preceding paragraph, the electrical conductance of the two tubes under various AFM-deformation angles were computed via the Landauer-Büttiker formula using a tight-binding code based on the non-equilibrium-Green's-Function [14]. The main results are summarized below [15]:

i) Even under significant AFM-deformation, the tubes remain all-hexagonal and each C-atom remains essentially sp^2-coordinated. However, conductance drops are much higher than similar tubes *bent* under mechanical duress. This is particularly true for the zigzag tube. Thus, at a deformation angle of 25°, the conductance for the (6, 6) tube drops by 5%, and that for the (12, 0) tube drops by a whopping four orders of magnitude.

ii) The difference in electrical response of CNTs to bending vs. AFM-deformations can be primarily attributed to a net elongation of the tube under the latter deformation, and no net stretching under bending. Thus, the drop in conductance in the AFM-deformation experiment can be mimicked in a simpler experiment in which the tube is subjected to a uniform tensile strain.

iii) The difference between the conductance behavior of armchair versus zigzag tubes can be attributed to the opening of a gap at the Fermi surface for a zigzag tube under stretch, while no such gap opens up for an armchair tube. Details are described elsewhere [15].

Currently we are simulating experiments in which the tubes are being placed on a "hard" surface (substrate) and pushed from the top with AFM tips. Preliminary investigations with AFM-tips represented by close-capped nanotube tips indicate that there are possibilities of chemical bonding between atoms of opposite walls of the nanotube itself, as well as between atoms of the AFM tip and the tube. This gives rise to interesting possibilities of electron hopping to and from the AFM tip, which might open up new pathways for electronic conduction.

4 METAL-OXIDE NANORIBBONS AS CHEMICAL SENSORS

Recent experiments with SnO_2 nanoribbons indicate that these are highly effective in detecting even very small

amounts of harmful gases like NO_2. Upon adsorption of these gases, the electrical conductance of the sample decreases by several orders of magnitude. More interestingly, it is possible to get rid of the adsorbates by shining UV light, and the electrical conductance is completely restored to its original value [16]. The experimental nanoribbons were synthesized using a novel approach based on thermal deposition. The resulting ribbons were several microns long, possessed a highly uniform crystalline order, exposed the (1 0 $\bar{1}$) and (0 1 0) surfaces normal to the growth direction (z-axis), with dimensions of 80-120 nm x 10-30 nm respectively.

Rutile SnO_2 is a wide-bandgap insulator ($E_{gap} \sim 3.6$ eV), which is effectively *n*-doped due to the departure from stoichiometry, primarily in the form of oxygen vacancies [17]. Electron withdrawing groups like NO_2 and O_2 are expected to deplete the conduction electron population in the nanoribbon, thereby leading to a decrease in electrical conductance. We have used first-principles DFT simulations with DMol[3] to investigate the binding geometries, binding energies, and charge transfer for three different adsorbing species: NO_2, O_2 and CO. Important results are summarized below:

i) NO_2 adsorption displays a very rich chemistry because it can either form a single bond to a surface Sn, or can adsorb in the bidented form through two single bonds to neighboring Sn-atoms. The doubly bonded NO_2 is 2-3 kcal/mol more stable than the single-bonded NO_2, and the binding energies are in general 4-5 kcal/mol higher on the (1 0 $\bar{1}$) surface than on the (0 1 0). Activation barrier between the doubly-bonded and single-bonded structures is expected to be low, which should make the NO_2 species mobile on the exposed faces, especially on the (0 1 0).

ii) When a second NO_2 is incident in the vicinity of an already-chemisorbed NO_2, one of the O-atoms of the second NO_2 breaks away and attaches to the chemisorbed NO_2, thus converting it to a surface NO_3 species. The bidented NO_3 group has a substantially higher binding energy, especially on the (1 0 $\bar{1}$) surface, and should not, therefore, be mobile.

iii) A CO likes to adsorb in the following manner: the C forms two single bonds to the surface -- one with a surface Sn and another with a bridging O, while the O of the CO forms a double bond to the C and sticks out of the surface. This way, the C-atoms attains its preferred 4-valency and the O has its bivalency satisfied.

iv) On a defect-free surface (i.e. surface with no O-vacancies), the O_2 molecules can only weakly physisorb. In this configuration, there is no charge transfer to the O_2, and therefore a nanoribbon surface without surface O-vacancies should be insensitive to atmospheric oxygen. However, at O-vacancy sites, the O_2 molecule has a strongly bound chemisorbed structure in the form of a peroxide bridge.

v) Both NO_3 groups and chemisorbed O_2 (at O-vacancy sites) accept significant amount of electronic charge from the surface. Therefore, such adsorbates should lead to the lowering of electrical conductance of the sample. CO, on the other hand, donates a moderate amount of electrons to the surface, and is therefore expected to increase the electrical conductance. Such effects have been confirmed in direct experimental measurements of sample conductance.

vi) Synchrotron measurements using X-ray Absorption Near-Edge Spectroscopy (XANES) has recently confirmed the abundance of NO_3 species on the nanoribbon surface following NO_2 adsorption.

Details are described elsewhere [18].

REFERENCES

[1] *http://www.accelrys.com/mstudio/dmol3.html*; B. Delley, *J. Chem. Phys* 92, 508, 1990; *J. Phys. Chem.*100, 6107, 1996; *Int. J. Quantum Chem.* 69, 423, 1998; *J. Chem. Phys.*113, 7756, 2000.

[2] S. Iijima, Nature 354, 56, 1991.

[3] Articles on nanotubes in Physics World 13, Issue 6, pp. 29-53, 2000.

[4] W. A. de Heer, A. Chatelain, and D. Ugarte, Science 270, 1179, 1995; A. G. Rinzler *et al.*, Science 269, 1550, 1995; P. G. Collins and A. Zettl, Appl. Phys. Lett. 69, 1969, 1996; Y. V. Gulyaev *et al.*, J. Vac. Sci. Technol. B 15, 422, 1997; S. Fan *et al.*, Science 283, 512, 1997; O. M. Küttel, O. Groenig, C. Emmenegger, and L. Schlapbach, Appl. Phys. Lett. 73, 2113, 1998; M. J. Fransen, Th. L. van Rooy, and P. Kruit, Appl. Surf. Sci. 146, 312, 1999.

[5] K. A. Dean, P. von Allmen, and B. R. Chalamala, J. Vac. Sci. Technol. B 17, 1959, 1999.

[6] A. Maiti, C. J. Brabec, C. Roland, and J. Bernholc, Phys. Rev. Lett. 73, 2468, 1994.

[7] A. Maiti, J. Andzelm, N. Tanpipat, and P. Von Allmen, Phys. Rev. Lett. 87, 155502, 2001.

[8] M. Grujicic *et al.*, Appl. Surf. Sci., *in press*, 2003.

[9] T. W. Tombler *et al.*, Nature 405, 769, 2000.

[10] L. Liu *et al.*, Phys. Rev. Lett. 84, 4950, 2000.

[11] A. K. Rappe, C. J. Casewit, K. S. Colwell, W. A. Goddard, and W. M. Skiff, J. Am. Chem. Soc. 114, 10024, 1992.

[12] The contact region was defined by a unit cell plus one atomic ring (a total of 36 and 60 atoms for the armchair and the zigzag tube respectively) at each end of the tube.

[13] Z. Lin and J. Harris, J. Phys.: Condens. Matter 4, 1055, 1992; X. P. Li, J. W. Andzelm, J. Harris, and A. M. Chaka, American Chemical Society, Anaheim Symposium (1995).

[14] A. Svizhenko, M. P. Anantram, T. R. Govindan, B. Biegel, and R. Venugopal, J. Appl. Phys. 91, 2343, 2002.

[15] A. Maiti, A. Svizhenko, and M. P. Anantram, Phys. Rev. Lett. 88, 126805, 2002.

[16] M. Law, H. Kind, F. Kim, B. Messer, P. Yang, *Angew. Chem.* 41, 2405, 2002.

[17] C. G. Founstad and R. H. Rediker, J. Appl. Phys. 42, 2911, 1971.

[18] A. Maiti, J. Rodriguez, P. Kung, and P.Yang, Phys. Rev. Lett., *submitted.*